frontiers in Materials

ORIGINAL RESEARCH
published: 05 August 2021
doi: 10.3389/fmats.2021.686353

Structural Study of the Hydration of Lipid Membranes Upon Interaction With Mesoporous Supports Prepared by Standard Methods and/or X-Ray Irradiation

Benedetta Marmiroli[1]*, *Barbara Sartori*[1], *Adriana R. Kyvik*[2,3], *Imma Ratera*[2,3] and *Heinz Amenitsch*[1]*

[1]Institute of Inorganic Chemistry, Graz University of Technology, Graz, Austria, [2]Institute of Materials Science of Barcelona (ICMAB-CSIC), Campus UAB, Bellaterra, Spain, [3]Networking Research Center on Bioengineering, Biomaterials and Nanomedicine (CIBER-BBN), Campus UAB, Bellaterra, Spain

OPEN ACCESS

Edited by:
P. Davide Cozzoli,
University of Salento, Italy

Reviewed by:
Angela Agostiano,
University of Bari Aldo Moro, Italy
Piotr Warszynski,
Jerzy Haber Institute of Catalysis and Surface Chemistry (PAN), Poland

***Correspondence:**
Benedetta Marmiroli
benedetta.marmiroli@tugraz.at
Heinz Amenitsch
heinz.amenitsch@tugraz.at

Specialty section:
This article was submitted to Colloidal Materials and Interfaces, a section of the journal Frontiers in Materials

Received: 26 March 2021
Accepted: 02 July 2021
Published: 05 August 2021

Citation:
Marmiroli B, Sartori B, Kyvik AR, Ratera I and Amenitsch H (2021) Structural Study of the Hydration of Lipid Membranes Upon Interaction With Mesoporous Supports Prepared by Standard Methods and/or X-Ray Irradiation. Front. Mater. 8:686353. doi: 10.3389/fmats.2021.686353

Mesoporous materials feature ordered tailored structures with uniform pore sizes and highly accessible surface areas, making them an ideal host for functional organic molecules or nanoparticles for analytical and sensing applications. Moreover, as their porosity could be employed to deliver fluids, they could be suitable materials for nanofluidic devices. As a first step in this direction, we present a study of the hydration of 1-palmitoyl-2-oleoyl-sn-glycero-3-phosphocholine (POPC) model lipid membranes on solid mesoporous support. POPC was selected as it changes the structure upon hydration at room temperature. Mesoporous films were prepared using two different templating agents, Pluronic P123 (PEO–PPO–PEO triblock copolymer where PEO is polyethylene oxide and PPO is polypropylene oxide) and Brij 58 ($C_{16}H_{33}(EO)_{20}OH$ where EO is ethylene oxide), both following the conventional route and by X-ray irradiation via deep X-ray lithography technique and subsequent development. The same samples were additionally functionalized with a self-assembly monolayer (SAM) of (3-aminopropyl)triethoxysilane. For every film, the contact angle was measured. A time resolved structural study was conducted using *in situ* grazing incidence small-angle X-ray scattering while increasing the external humidity (RH), from 15 to 75% in a specially designed chamber. The measurements evidenced that the lipid membrane hydration on mesoporous films occurs at a lower humidity value with respect to POPC deposited on silicon substrates, demonstrating the possibility of using porosity to convey water from below. A different level of hydration was reached by using the mesoporous thin film prepared with conventional methods or the irradiated ones, or by functionalizing the film using the SAM strategy, meaning that the hydration can be partially selectively tuned. Therefore, mesoporous films can be employed as "interactive" sample holders with specimens deposited on them. Moreover, thanks to the possibility of patterning the films using deep X-ray lithography, devices for biological studies of increasing complexity by selectively functionalizing the mesopores with biofunctional SAMs could be designed and fabricated.

Keywords: deep X-ray lithography, mesoporous silica thin films, lipid membrane hydration, small-angle X-ray scattering, contact angle, molecular surface functionalization

INTRODUCTION

The ability to manipulate small amounts of fluids, in particular in the field of medicine and biology, where some samples are available in small quantities and/or very expensive, has boosted the development of both microfluidics and, more recently, nanofluidics (Xu, 2018; Scheler et al., 2019; Craig et al., 2020). A further improvement of micro/nanofluidic systems for handling and detecting (bio)samples would consist in the insertion of materials presenting desired functionalities in chosen areas of the devices. Mesoporous thin films are materials synthesized through a bottom-up process that can be integrated into microdevices using top-down fabrication techniques. They are composed of an inorganic compound and a templating agent that controls the structure morphology such as the pore network or pore size during self-assembly. The films, usually produced by dip or spin coating of the precursor solution and subsequent thermal treatment, present a thickness around 100–500 nm and include uniform and connected pores of 2–50 nm (Grosso et al., 2004; Innocenzi and Malfatti, 2013). Among mesoporous materials, our attention was focused on mesoporous silica, which is biocompatible and can be further functionalized using molecular SAMs by a silane coupling chemistry (Ketteler et al., 2008; Seras-Franzoso et al., 2012; Sánchez et al., 2013; Tatkiewicz et al., 2013). It is known that silica is hydrolyzed in water, and it undergoes degradation with time. However, a recent study demonstrated that dissolution kinetics depend on the accessible surface area, the surrounding media composition, the residual surfactant molecules inside the pores, and their functionalization (Bindini et al., 2020).

Adding the possibility of micropatterning thin films, it would allow for the fabrication of microdevices, for example, for biosensing or biocatalysis (Magner, 2013; Lei et al., 2020).

Among the different lithographic techniques, deep X-ray lithography (DXRL) was shown to be an effective top-down method to pattern sol–gel materials (Marmiroli and Amenitsch, 2012; Innocenzi et al., 2014). DXRL is based on the exposure of materials to synchrotron high-energy X-rays (2–30 keV), leading to chemical and structural changes. If the irradiation is conducted through a suitable mask, microstructures can be obtained with high aspect ratio (ratio between height and minimum lateral dimension) and 200 nm lateral resolution (Tormen et al., 2013). In previous research, mesoporous silica films were patterned using DXRL where the X-rays simultaneously increase the polycondensation of the exposed silica while partially removing the surfactant (Falcaro et al., 2008; Falcaro et al., 2009; Innocenzi et al., 2011).

The possibility of employing mesoporous silica films in micro/nanofluidic devices is still under investigation. They were already used as support for lipid membranes, increasing their mechanical stability and leaving space under the membrane, for example, for transmembrane proteins. Lipid membranes could therefore be studied with characterization techniques such as AFM, quartz crystal balance, and electrochemical impedance spectroscopy (Claesson et al., 2010; Claesson et al., 2011; Zhou et al., 2020). Synthetic lipid bilayers are widely studied, as they can be employed to mimic cell membranes, making them very attractive in fields such as drug delivery and biosensing. As mesoporous silica films are subject to water filling and condensation as a function of relative humidity (RH) (Dourdain and Gibaud, 2005), this effect could be exploited to deliver water through the pores.

In this work, we present our study of the hydration of lipid membranes supported on mesoporous silica films and their comparison with the ones deposited on silicon.

Among the lipid membranes, 1-palmitoyl-2-oleoyl-sn-glycero-3-phosphocholine (POPC) was chosen, as its structure is changing as a function of humidity in three different lamellar phases (Katsaras et al., 1993). In order to follow the evolution of the structure with increasing RH, grazing incidence small-angle X-ray scattering (GISAXS) measurements were conducted, as this technique allows for *in situ* observation of structural features typically between 1 and 100 nm and has already been widely employed to examine POPC under different conditions among which RH changes (Pabst et al., 2000; Amenitsch et al., 2004; Rappolt et al., 2004). GISAXS had also been previously applied to investigate the structure and the porous properties of mesoporous films, in particular the contraction of pores in mesoporous films due to capillary condensation with the rise of humidity (Gibaud et al., 2004; Grosso et al., 2004; Dourdain et al., 2005; Sharifi et al., 2014).

Here, mesoporous silica films were prepared using two surfactants, Brij 58 and P123, resulting in different pore dimensions and lattice arrangement. After sol–gel preparation and deposition on the silicon substrate, the following protocols were applied: 1) thermal treatment with the standard preparation route, 2) irradiation and development via DXRL, and 3) both treatments. The effect of film functionalization using molecular SAMs with subsequent increase of hydrophobicity was evaluated. The films were characterized by both measuring the contact angle (CA) and using GISAXS. Then, their structural change with increasing humidity was investigated using *in situ* GISAXS in a custom-made humidity chamber. After the deposition of POPC, *in situ* GISAXS measurements were repeated in order to check the hydration of POPC. The results were compared with the ones obtained by depositing POPC on a silicon wafer.

EXPERIMENTAL DETAILS

Preparation of Mesoporous Silica Films

Tetraethyl orthosilicate (TEOS), ethanol (EtOH) 99.8%, and HCl were purchased from Carl Roth GmbH + Co. KG (Karlsruhe, Germany); Brij 58 and Pluronic P123® were purchased from Merck KGaA (Darmstadt, Germany). All reagents were used as supplied.

Two kinds of mesoporous silica films were synthesized, based on the different templating surfactants.

The first batch of samples was prepared using Brij 58, adapting the recipe proposed by Fuertes et al. (2007) as follows.

TEOS (2.1 g), ethanol (6 g), water, and concentrated HCl were mixed at room temperature for 1 h. Brij 58 (0.56 g) was dissolved

TABLE 1 | List of samples with different treatments subject to investigation.

Surfactant	Irradiation + development	Thermal treatment	Functionalization
Brij 58		x	
Brij 58		x	x
Brij 58	x		
Brij 58	x		x
Brij 58	x	x	
Brij 58	x	x	x
P123		x	
P123		x	x
P123	x		
P123	x		x
P123	x	x	
P123	x	x	x

in 5 g of ethanol. After 1 h, the two solutions were stirred together for 1 h at room temperature. The pH was checked to be lower than 3 before spin coating. The final molar composition of the solution was 1 TEOS:0.05 Brij 58:5.2 H_2O:24 EtOH:0.28 HCl.

For the second batch, Pluronic 123 (P123) was employed, according to the recipe proposed by Yan et al. (2007) as follows.

TEOS (1.75 g), ethanol (1 g), and 1.25 ml of 0.0025 M HCl were mixed and stirred for 1 h at room temperature. 0.584 g of P123 was dissolved in 26.8 g of ethanol at room temperature with vigorous stirring. After 1 h, the surfactant solution was added to silica and mixed for 1.5 h. 1.93 ml of acidified water was added to the solution and stirred for 15 min. The pH was checked and adjusted to 2.5 with concentrated HCl.

In the following, the mesoporous silica films will be identified by the surfactants Brij 58 and P123.

Both film batches were processed via spin coating on silicon wafers (Laurell WS-650_MZ-23 NPPB, Laurell Technologies Corporation, United States), for 1 min at 800 rpm.

After spin coating, the samples were subject to three different treatments:

1) Thermal treatment.
2) X-ray irradiation and development.
3) X-ray irradiation and development followed by thermal treatment.

After every kind of processing, the films were first characterized and then further functionalized with molecular SAMs in order to change their hydrophilicity.

The list of the different mesoporous films studied in this work is shown in **Table 1**.

CA and GISAXS measurements were performed on each film. The samples were selected in order to study the following:

1) The effect of different pore arrangement and dimensions.
2) The effect of irradiation compared to standard thermal treatment.
3) The effect of functionalization of the pores.

After CA and GISAXS measurements, a lipid membrane was deposited on each type of mesoporous film, and GISAXS was performed again. In the following, a more detailed description of every procedure is given.

Thermal Treatment

This is the standard method to both remove the surfactant (P123 or Brij 58) and crosslink the silica of the precursor (TEOS). It was performed in an oven (Carbolite Oven, with Eurotherm 2416 control) at different temperatures.

For Brij 58, a temperature ramp was set to achieve 350°C in 1 h, and the value was subsequently kept constant for 2 h.

For P123, a temperature of 450°C was reached in 1 h, and then it was maintained constant for 30 min.

X-Ray Irradiation

DXRL is based on the fact that some materials (defined as resists) undergo a dissolution rate change in a specific solvent (called developer) when exposed to X-rays. Resists are exposed to synchrotron radiation in a controlled way (Becker et al., 1986; Romanato et al., 2006). If an X-ray mask, composed of an absorbing material (gold) and an X-ray transparent supporting membrane (thin layer of graphite, or SiNx or TiO or SU8...) is inserted between X-rays and the sample, then it is possible to obtain micropatterning with good lateral resolution (200 nm) and comparatively high resist thickness with respect to all other lithographic techniques. In the case of mesoporous silica films, silica condensation is induced together with the breakage of the surfactant. Therefore, mesoporous silica is a negative resist. The scheme of the process is shown in **Figure 1A**.

The samples were irradiated at the DXRL beamline of the Elettra synchrotron radiation source (Pérennès et al., 2001; Pérennès and Pantenburg, 2001) using a Dex02 Jenoptik scanner (Jenoptik AG, Jena, Germany). The storage ring was working at 2 GeV with a current of 310 mA. The irradiation occurred through a white beam of energy range 2–20 KeV and peak around 6 KeV. Brij 58 samples received an energy per unit surface (dose) of 68 J/cm^2, while the P123 ones got 272 J/cm^2. The dose had been previously selected by performing an irradiation series with increasing energy to determine the minimum irradiation dose for which the structure was retained after development (Steinberg et al., 2021).

The films were exposed immediately after spin coating and, just after exposure, developed to remove the templating agent, as

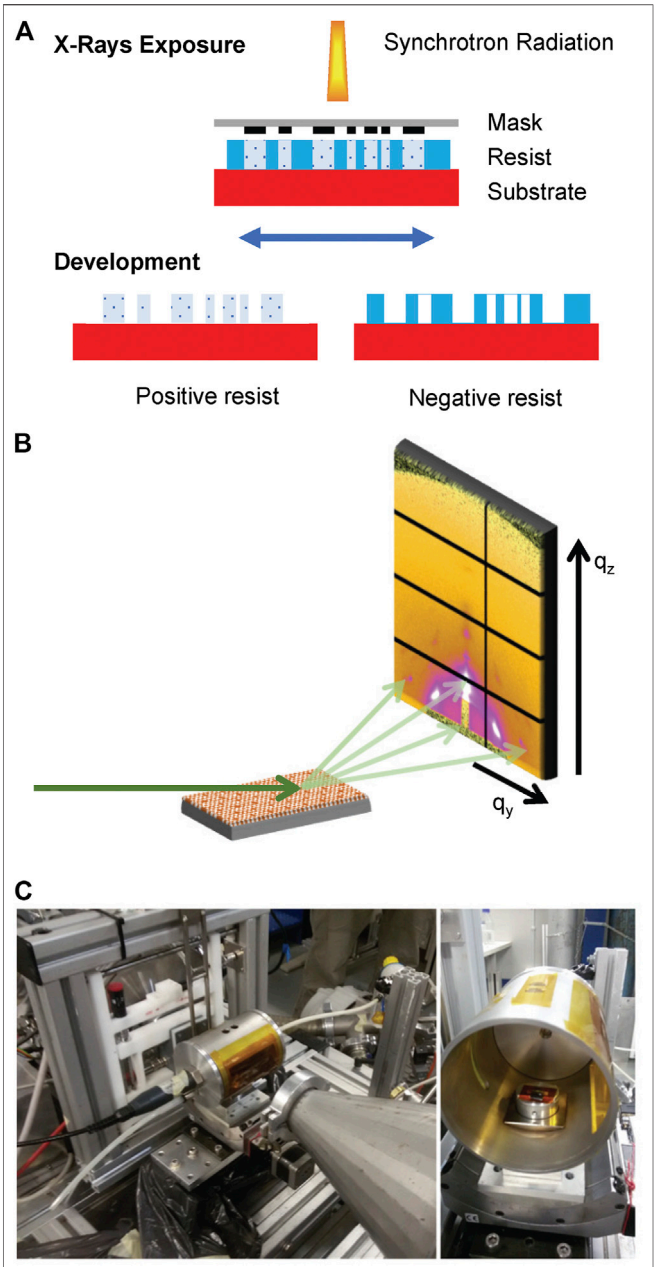

FIGURE 1 | (A) Scheme of the DXRL process, showing the irradiation of both positive and negative resists with synchrotron X-rays. **(B)** Graphic representation of the GISAXS experiment. X-rays hit the sample at grazing angle, and the scattered photons are collected at the detector. **(C)** Humidity sample chamber mounted at the Austrian SAXS beamline at Elettra.

aging of the sol–gel would prevent the removal of the surfactant after irradiation.

For Brij 58, the developer solution consisted of ethylene glycol: acetone:ethanol:water = 1:1:1:1 (v/v) and the samples were immersed for 10 min.

For P123, the solution was composed of ethylene glycol:acetone: ethanol = 4:2:1 (v/v). The development time was 30 min.

In both cases, after development, the films were rinsed in ethanol and dried with nitrogen. Some samples were thermally treated following the procedures explained earlier, in order to assure that all surfactant had been completely removed, as already evidenced for Brij 58 by Steinberg et al. (2021).

Self-Assembly Monolayer Functionalization of the Mesoporous Films

The mesoporous silica thin films were functionalized with (3-aminopropyl)triethoxysilane (APTES) (Merck KGaA, Darmstadt, Germany), commonly used for surface silanization. It was chosen as amino terminal functional groups can be employed as linkers to further functionalize the films with bio-macromolecules. A post-grafting functionalization was selected because the number of available functional groups is higher than the one obtained when the precursors are co-condensed during the mesoporous material synthesis (Calvo et al., 2009). The scheme of the first mesoporous layers in films functionalized using SAMs via post-grafting is shown in **Supplementary Figure S1**.

The functionalization protocol consisted in the following steps:

1) Cleaning of the substrates by immersion for 5 min in acetone, 5 min in chloroform, and 5 min in isopropanol (all from Merck KGaA, Darmstadt, Germany), then rinsing in Milli-Q water, and drying with nitrogen.
2) Plasma treatment with O_2 at a power of 20 W for 10 min to eliminate residues.
3) Immersion in dry toluene solution (Merck KGaA, Darmstadt, Germany) containing 1 mM APTES overnight at 80°C under inert atmosphere.
4) Rinsing in toluene and ethanol.

Deposition of 1-Palmitoyl-2-oleoyl-sn-glycero-3-phosphocholine Lipid Membrane

POPC (Avanti Polar Lipids, Alabaster, AL, United States) was dissolved (10% w/w) in isopropyl alcohol (Rotisolv, >99.95%, Carl Roth GmbH + Co. KG). A suitable volume was dispensed on the mesoporous thin film with a micropipette and let undisturbed until dry (Tristram-Nagle et al., 1993; Claesson et al., 2010). Once dry, the samples were stored at room temperature in vacuum for at least 16 h, to completely evaporate the residual solvent, and removed from the vacuum chamber just before the measurement.

Contact Angle Measurements

The CA was determined using a Drop Shape Analyzer 100 (KRÜSS GmbH, Hamburg, Germany) through the drop shape analysis method. A 2 µL drop of ultra-pure water was placed on each mesoporous film to obtain the CA between the substrate and the liquid. All measurements were performed in the same conditions. For each substrate, three trials were conducted, with two fits each. The CA of each substrate was obtained by calculating the average. Measurements of non-functionalized and

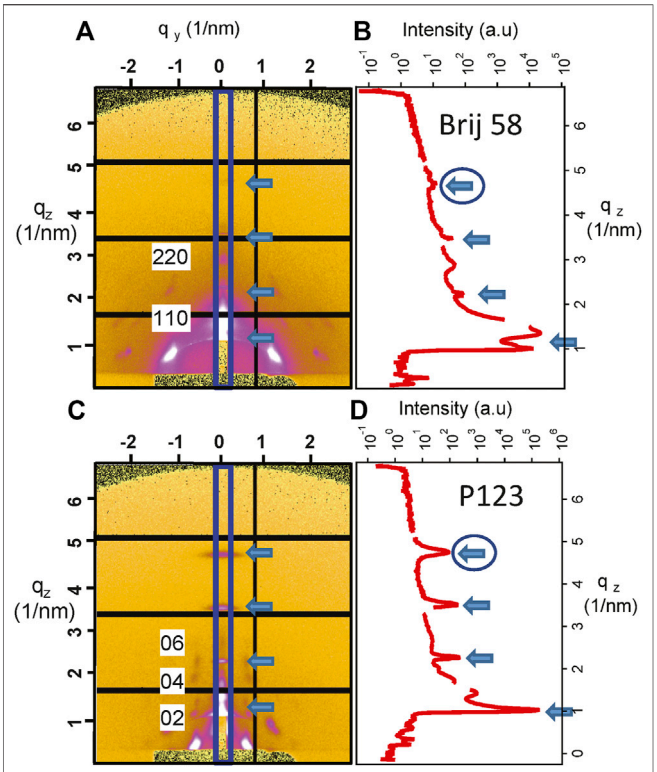

FIGURE 2 | (A) GISAXS image and **(B)** I–q_z patterns corresponding to the vertical cut evidenced by the rectangle for mesoporous silica prepared with Brij 58 and calcined after POPC deposition. The distorted (110)-oriented body centered cubic structure is evident and partially indexed along the q_z direction. **(C)** Image at the detector and **(D)** I–q_z patterns corresponding to the vertical cut evidenced by the rectangle for mesoporous silica prepared with P123 and calcined after POPC deposition. The distorted hexagonal structure is evident and indexed along the q_z direction. The arrows indicate the contribution of POPC, and the circled ones define the peaks that were used for the determination of the POPC phase transition.

SAM-functionalized silicon wafers were performed for comparison.

Grazing Incidence Small-Angle X-Ray Scattering Measurement

In GISAXS technique, a monochromatic X-ray beam hits the sample at a low angle. A 2D detector measures the scattered photons' intensity in the directions parallel (q_y) and perpendicular (q_z) to the sample surface (Renaud et al., 2009). From the 2D image on the reciprocal space, it is possible to determine both the dimension and arrangement of the pores of the mesoporous materials (Grosso et al., 2004) and the structure of the lipid membrane (Amenitsch et al., 2004; Rappolt et al., 2004). The scheme of the GISAXS experiment is shown in **Figure 1B**.

GISAXS measurements were performed at the Austrian SAXS beamline at Elettra (Amenitsch et al., 1997). The wavelength was λ = 0.154 nm, and 2D GISAXS patterns were collected with a Pilatus3 1M detector (Dectris, Baden, Switzerland) at a grazing angle of 0.4°. The angular scale of the detector was calibrated with silver behenate. After every measurement, the detector image was processed using SAXSDOG, a software program for automatic data reduction developed at the Austrian SAXS beamline (Burian et al., 2020). In the present case, the diffraction patterns of vertical cut q_z in the out-of-plane direction were considered for data analysis selecting the region (10 pixels) evidenced in **Figure 2A**. The detector distance was defined to have q_z in the range 0.31–6.8°nm^{-1}.

The experiments were conducted at controlled relative humidity (RH), defined as the ratio of the water vapor pressure to the saturation vapor pressure at a given temperature. The chamber is described by Sharifi et al. (2014) and shown in **Figure 1C**. It is composed of a metal cylinder equipped with two Kapton windows (13 μm thickness) to let the incident and the scattered beam pass through. Humidity is controlled by mixing dry (<3% RH) and humid (>95% RH) air produced with a supersonic humidifier in a mixer chamber and then flowing the mixture in the cell. A humidity sensor inside the chamber in connection with a proportional integral derivative (PID) controller is used to set the requested RH. The temperature was constant at 25 ± 1°C.

All samples listed in **Table 1** were measured at RH = 15% to determine the unit cell parameters (shown in **Supplementary Figure S1**). Then, the scattering pattern was collected while increasing the relative humidity from 15 to 75%, at a rate of 0.5%/min. The exposure time was set to 10 s every minute.

The specimens were then covered with POPC films following the procedure in *Deposition of 1-Palmitoyl-2-oleoyl-sn-glycero-3-phosphocholine Lipid Membrane* and underwent the same RH ramp while acquiring images for 3 s every minute to avoid radiation damage of the lipid membrane.

In this way, we could decouple the behavior of the mesoporous material from the one of the deposited POPC.

After completing the measurement, POPC was removed from the mesoporous samples by washing in isopropyl alcohol and dried in a vacuum chamber for at least 24 h. Then, SAM functionalization with APTES was performed as described in *Self-Assembly Monolayer Functionalization of the Mesoporous Films*. The same GISAXS experiments were conducted as for not functionalized samples to determine the unit cell parameters and the effect of humidity increase on functionalized mesoporous films alone. Afterward, the samples were dried in vacuum. Subsequently, POPC was deposited and the humidity was increased again to examine the lipid membrane hydration.

RESULTS AND DISCUSSION

Contact Angle

As a first approach to investigate the hydrophilicity/hydrophobicity of the prepared surfaces, the contact angle was determined. The results for each sample are given in **Table 2**.

Although the standard deviation is quite high, we found that all samples without functionalization are hydrophilic, following the classical definition, as their contact angle is less than 90° (Law, 2014). As expected, functionalization increases hydrophobicity,

TABLE 2 | Contact angle (CA) of mesoporous materials prepared with two surfactants and subject to different treatments.

Sample description	CA (st dev)	CA (st dev) with APTES
Silicon	36.3° (1.42)	64.5° (0.89)
Brij 58 thermal treatment	77° (3.39)	88.23° (1.43)
Brij 58 irradiation and development	69° (3)	91.87° (0.46)
Brij 58 irradiation, development, and thermal treatment	73.7° (7.1)	84.267° (3.78)
P123 thermal treatment	70.6° (4.7)	89.4° (0.57)
P123 irradiation and development	78.8° (1.12)	87.3° (1.42)
P123 irradiation, development, and thermal treatment	78.6° (2.28)	82.3° (4.69)

as it replaces some of the -SiOH surface sites with more hydrophobic groups like $-(CH_2)_3NH_2$ of the APTES molecules (Calvo et al., 2009).

Grazing Incidence Small-Angle X-Ray Scattering Measurement

The representative detector images for mesoporous materials are shown in **Figure 2A** for Brij 58 and **Figure 2C** for P123 calcined films, respectively. The indexing of the peaks is limited to the most noticeable spots along the vertical cut, to evidence the position of the mesoporous silica peaks.

The diffraction patterns ($I–q_z$) of the out-of-plane cuts are presented in **Figures 2B,D**. The arrows indicate the contribution which is unequivocally related to the POPC lipid membrane. The circle highlights the peak that has been considered to demonstrate the phase transition of POPC upon humidity change. The diffraction peaks in **Figure 2A** demonstrate the orthorhombic *Fmmm* structure of the Brij 58 templated silica mesopores derived from the distorted (110)-oriented body centered cubic *Im3m* to which the indexing is referred (Crepaldi et al., 2003; Voss et al., 2014). The peaks in **Figure 2C** show the hexagonal arrangement of the pores in the P123 templated mesoporous film (Sharifi et al., 2014).

Mesoporous Silica Films With and Without Self-Assembly Monolayer Functionalization

The unit cells considered for the calculation of the structure parameters are shown in **Supplementary Figure S2**, and the unit cell parameters for every kind of sample are reported in **Supplementary Table S1**. In the case of mesoporous materials prepared using the Brij 58 surfactant, the *Fmmm* cells were around b = 6 nm in the direction parallel to the substrate and a = 3.8 nm in the perpendicular direction, indicating a strong shrinkage of the original mesoporous structure upon both thermal treatment and irradiation. The samples subject to both irradiation and thermal treatment presented the highest contraction of the original structure (a = 2.8 nm).

Similar considerations can be drawn for the *p6m* structure of the mesoporous materials prepared with surfactant P123. In this case, the unit cell parameters were bigger: b = 13–14 nm, a = 14–15 nm. These data are consistent with the findings presented by Ganser et al. (2016) relative to mesoporous materials prepared with the same surfactant and a similar thermal treatment. The effect of both irradiation and thermal treatment leads to a further distortion and a = 10.1 nm.

The influence of the increase of RH (%) on the mesoporous silica structure was evidenced using the following procedure:

1. The intensity of peak (110) for mesoporous materials prepared with Brij 58, and of peak (200) for the ones with P123, was directly calculated from the detector image integrating the 2D peak area.
2. The intensity change due to the increase of RH was normalized to the initial value of intensity for the dry sample at RH = 15%. In this way, the behavior of the different mesoporous materials could be compared.

The normalized intensity changes versus RH for all samples with their corresponding treatment (thermally treated samples, irradiated and developed, irradiated/developed/thermally treated) are shown in **Figure 3**. In detail, Figures 3(A) and (C) refer to the mesoporous silica prepared with the Brij 58 surfactant, respectively, without and with functionalization; Figures 3(B) and (D) describe the behavior of samples with surfactant P123 in the absence and presence of APTES SAMs.

Mesoporous silica films prepared with both surfactants without further functionalization had similar behavior in spite of different dimensions and arrangement of the pores. This is in line with the research conducted by Ceratti et al. (2015), who found that there is not direct correlation between the mesopores' dimension or arrangement and their capillary filling rate.

For both kinds of structures, only the film condensed regime was present in the RH range 15–75%, meaning that water molecules form a thin film on the pore walls (Huber, 2015). A hint of the onset of capillary condensation at an RH>70% could be observed for thermally treated samples (both with and without irradiation and development). As far as mesoporous silica prepared with P123 and thermally treated is concerned, the measurement agreed well with the results presented by Sharifi et al. (2014) and Ganser et al. (2016) for a thermally treated mesoporous material prepared with a similar recipe.

The behavior of not functionalized films prepared by irradiation and development, particularly those templated by the P123 surfactant, shows a different trend with nearly no change with RH. On the contrary, the functionalization with APTES SAMs had an influence on the performance of the mesoporous films with RH, and it affected differently the structures derived from the two surfactants.

Functionalized samples prepared using Brij 58 and undergoing a thermal treatment (with and without irradiation) presented a capillary condensation starting at RH = 30–35%. The

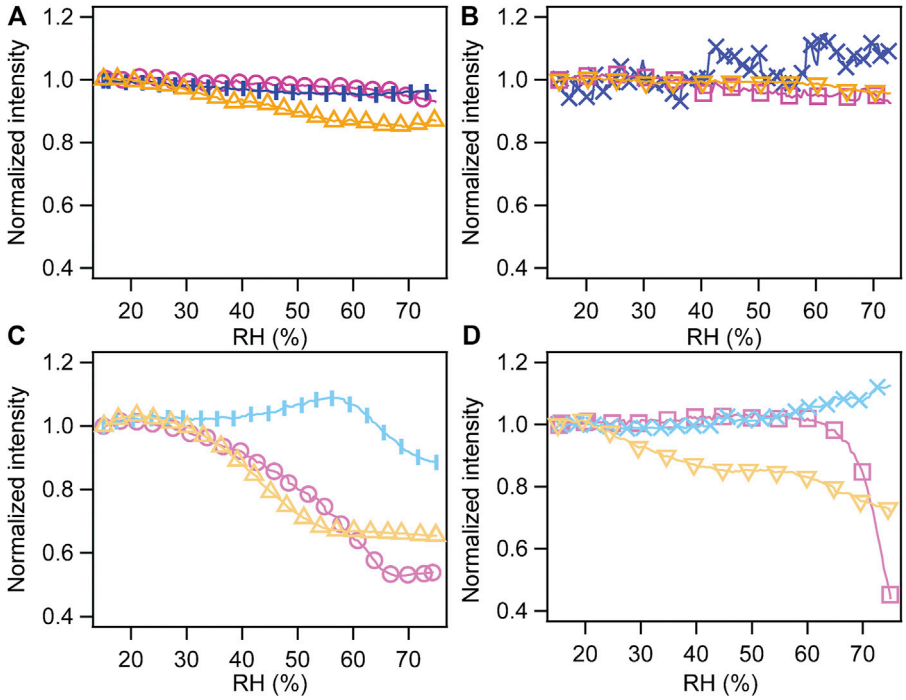

FIGURE 3 | Normalized intensity of peak (110) of the cubic phase (Brij 58) and of peak (200) of the hexagonal phase (P123) as a function of RH. **(A)** Mesoporous silica prepared with surfactant Brij 58. **(B)** Mesoporous silica with the P123 templating agent. **(C)** Mesoporous silica with Brij 58 functionalized with APTES. **(D)** Mesoporous silica with P123 functionalized with APTES. Pink curves represent thermally treated samples (circles, Brij 58; squares, P123), blue ones represent irradiated and developed ones (vertical bar markers, Brij 58; x markers, P123), and yellow ones represent irradiated, developed, and thermally treated ones (triangles with tip up, Brij 58; triangles with tip down, P123).

irradiated film had a drop of intensity at a higher RH (around 60%) indicating an onset of capillary condensation, even if the complete filling of the pores does not occur.

As far as the functionalized films obtained employing P123 are concerned, only the thermally treated one without irradiation displayed a clearly defined capillary condensation starting at around RH = 60%. The irradiated film presented the same behavior as the not functionalized one, suggesting that development after irradiation did not result in a full pore opening. The films subject to irradiation, development, and thermal treatment exhibited a hydration mechanism which is more difficult to interpret but still showed that water is entering at least partially the pores.

The behavior of mesoporous materials thermally treated and functionalized with APTES was opposite to the one described by Khalil et al. (2020) for functionalized mesoporous materials, where the onset of capillary condensation with RH increases with hydrophobicity. However, both the used (1,1,2H,2H-perfluorooctyldimethylchlorosilane) molecule, which is much longer and more hydrophobic than APTES, and the functionalization procedure were different. We believe that, in our case, the functionalization produced a dense layer of amino terminal groups inside the pores that led to a steric reduction of their dimension and thus to the capillary filling for lower values of RH (see **Supplementary Figure S1**).

Mesoporous Silica Films With and Without Functionalization Plus 1-Palmitoyl-2-oleoyl-sn-glycero-3-phosphocholine

It is known from the literature that, at 20°C, POPC presents three different lamellar phases depending on RH (%) (Katsaras et al., 1993):

L_δ at RH = 0–15% with d-spacing = 5.47 nm at RH = 0%
L_β at RH = 15–50% with d-spacing = 5.74 nm at RH = 40%
L_α at RH = 65–100% with d-spacing = 5.12 nm at RH = 100%

The measurements described in this work were conducted at 25°C, but both the behavior and the d-spacing were similar. To confirm it, POPC was deposited on bare Si with and without functionalization with the procedure described in *Deposition of POPC Lipid Membrane*, and an *in situ* GISAXS experiment was performed at increasing RH. Then, mesoporous samples with POPC were measured and compared to silicon ones. The I–q_z patterns for each humidity ramp have been plotted together at increasing RH. An example is shown in **Figure 4A** for the sample prepared using surfactant P123, irradiated and developed. The selected q-range is the one relative to the fourth order of the POPC lamellar phase, and it was chosen to avoid the influence of the signal of mesoporous silica dominating in the lower q-range (see also **Figure 2**). The lipid membrane undergoes a structural transition from the L_β phase, present at lower RH, to the L_α phase.

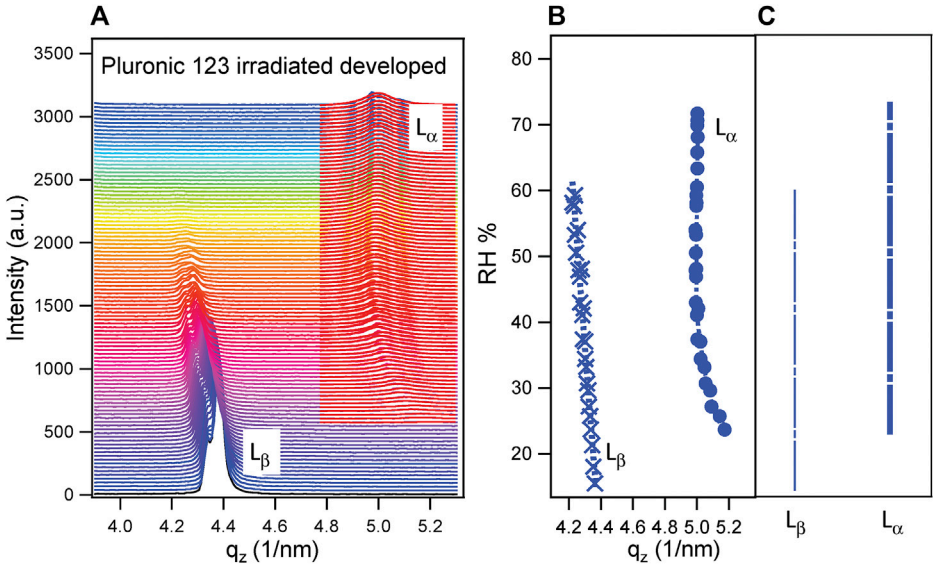

FIGURE 4 | (A) Out-of-plane pattern (I–q_z) at increasing RH for POPC deposited on a thin mesoporous silica film prepared with surfactant P123, irradiated and developed. The two phases L_β and L_α are shown, evidencing the structural transition of POPC upon increasing relative humidity. The red curves, superimposed to the measured ones in correspondence with the L_α phase, represent the Lorentzian fitting of the peaks of the lamellar phase. **(B)** q_z resulting from the Lorentzian fitting of the L_β phase (left) and L_α phase (right) as a function of RH (%). **(C)** Scheme of the RH (%) range of existence of the L_β phase (left) and L_α phase (right).

In the current case, both phases were coexisting for a certain RH range. The presence of two peaks in every phase, particularly evident in L_β, was due to a partial disorder of the deposited POPC. All peaks were fitted with a Lorentzian function (as shown for L_α), as Lorentzian distribution describes well the peak shape of smectic liquid crystalline systems (Rappolt, 2010). The resulting q_z for both phases as a function of RH (%) for the sample prepared with P123, irradiated and developed, is shown in **Figure 4B**. The RH (%) ranges of existence of the two phases are schematized in **Figure 4C**.

The d-spacing of the lipid membrane phases and its evolution with the increase of RH was calculated using the following formula for lamellar systems (Mangold, 1995):

$$d = 2\pi\left(\frac{l}{q}\right)$$

where l is the reflection order. In the present case, l = 4.

A summary of the results is shown in **Supplementary Figure S3**. The determined values agree with the ones reported in the literature.

A summary of the RH ranges for L_β and L_α phases for all samples is shown in **Figure 5**. The lines are correspondent to different substrates: the dashed ones are relative to the films prepared with the P123 surfactant (top) and the continuous ones represent the mesoporous films prepared using Brij 58 (middle). Thicker lines represent L_α phases, and thinner ones represent L_β. The shadowed areas with the letter A depict the APTES-functionalized samples. Colors refer to diverse treatments. The corresponding CA value is reported beside every sample. Two schemes showing the hydration of the lipid membrane with and without mesoporous film are also shown.

The lipid membrane hydration was evaluated mainly by considering the RH value at which the humid phase L_α appeared. In fact, the disappearing of L_β (dry phase) was more difficult to interpret, as POPC had been deposited via drop casting and its thickness in the different samples was not uniform, and the phase transition is related to water diffusion and to water availability across the thickness.

The following considerations can be drawn:

1) Mesoporous materials conveyed water to POPC through the pores, as in all cases the L_α phase (the hydrated one) occurred at a value of RH which was lower with respect to POPC deposited on bare Si. With Si, the onset of L_α started at RH around 40%, while with mesoporous materials, it occurred at about 20%.
2) It was confirmed that different surfactants do not lead to a drastic change of the behavior. P123 and Brij 58 mesoporous materials displayed a similar performance even if both the pore arrangement and the pore dimension were different (Ceratti et al., 2015).
3) In general, thermally treated samples conveyed more water than only irradiated ones. This is attributed to the fact that the developer solution was not able to efficiently open the pores, as already inferred from the lack of capillary condensation. This was most evident for the irradiated film prepared with surfactant P123. It looks like the pores are sterically blocked as they still contain the surfactant. Anyway, such films can still transfer water to the POPC membrane. One hypothesis, following Steinberg et al. (2021), was that pores are partially open and water flows at the interface between them and the lipid membrane. Water could also enter the interface between the silica and the surfactant or inside the

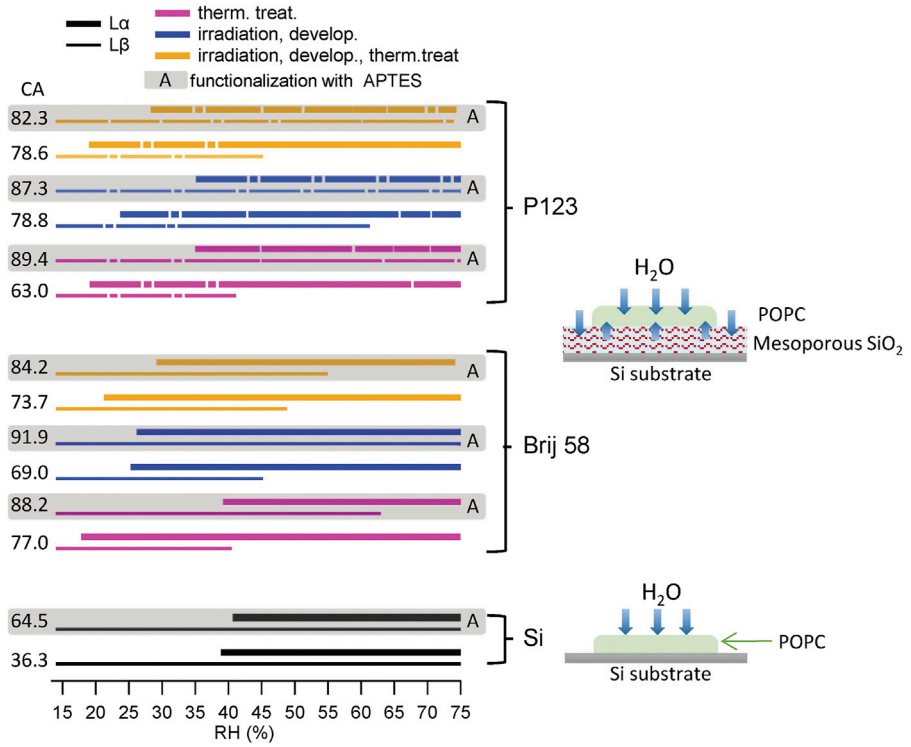

FIGURE 5 | Summary of the RH range of L_α and L_β phases for all samples and sketch of the hydration pathway. Black lines represent POPC deposited on silicon substrates **(bottom panel)**, continuous lines show the mesoporous films prepared using the Brij 58 surfactant **(middle panel)** and dashed lines show the films prepared with P123 **(top panel)**. Thicker lines correspond to L_α phases, and thinner ones correspond to L_β. The shadowed areas with the letter A indicate the samples functionalized with APTES. The pink colors **(bottom lines)** represent thermally treated samples, the blue ones **(middle lines)** represent irradiated and developed ones, and the yellow ones **(top lines)** represent irradiated, developed, and thermally treated ones. The CA value is reported beside the corresponding sample. Schemes of the hydration pathway of the lipid membrane deposited on Si and mesoporous thin films are, respectively, shown beside the corresponding substrates.

partially unconsolidated oxide. This could also explain why there was no visible change in the SAXS pattern of mesoporous silica with RH, as water is not replacing air in empty pores but the pores still contain surfactant; therefore, there is not electron density contrast.

4) The functionalization of Si with APTES did not lead to a big change of the hydration of POPC, even if the CA increased considerably.
5) APTES increased hydrophobicity of all mesoporous materials (as confirmed by the CA). This affected the hydration of the lipid membrane (evidenced by the onset of phase L_α). Lipid membranes supported on the APTES-functionalized mesoporous material exhibited a phase transition at RH values around 30%, lower than those at which it occurred when the lipid was deposited on bare silicon, but still at RH 5–10% higher than the one observed when POPC was drop casted on the not functionalized material. The disappearing of the dry phase L_β occurred at higher values for APTES-treated samples than the untreated ones. In some case, it did not even disappear. This partially contradicts the fact that capillary condensation, and therefore pore filling, occurs at a lower RH (%) for mesoporous materials functionalized with APTES, compared with the not functionalized ones.

When the lipid membrane is deposited on a hydrophilic surface (like silicon with a thin layer of native oxide), there is usually a hydration layer less than 2 nm thick that prevents the lipid from interacting strongly with the substrate (Kim et al., 2001). In this case, we speak of the continuous pore-spanning membrane. Functionalization with APTES favors the adsorption of the lipid membrane on the substrate, as the amino groups give a positive net charge to the substrate surface. This increases the electrostatic interaction with the negatively charged phosphate of the zwitterionic POPC headgroups, leading to a hybrid pore-spanning membrane (Leonenko et al., 2000; Bhattacharya et al., 2011). In this latter case, the fluidity of the resulting supported lipid membrane is not affected (Miyashita et al., 2018; Sun et al., 2020). As the sample prepared by drop casting presents thick layers, the structure and the hydration behavior of the lipid membrane depend only on the water content in the environment. This justifies why the behavior of POPC deposited on silicon substrates with and without functionalization is comparable. For mesoporous substrates, the amount of water delivered through the pores (in the liquid or vapor form) influences the onset of the humid phase (L_α) of POPC. The results show that the APTES-functionalized samples convey less water to the lipid membrane when compared to the

not functionalized ones, and this is in line with increased hydrophobicity of the surface and the pores.

From these measurements, it could be concluded that mesoporous films have an active effect on the hydration of supported POPC. The shift of the onset of L_α phase of POPC occurs as the water hydrates the lipid membrane also through the pores of the mesoporous materials. This is caused by the osmotic pressure due to the different water activity (chemical potential) in the lipid membrane and the surrounding environment (Milhaud, 2004). The hydration source can be at both the liquid and vapor phases. In the present case, there is vapor phase outside the mesopores due to an increase of RH (%). Inside the pores, the mechanism is more complex. The main contribution is from the vapor phase, as the anticipated onset of L_α is decoupled from the capillary condensation of water inside the pores. In the range of RH (%) where L_α appears, mesoporous films are in the condensed regime, where the molecules form a thin film of water on the pore walls. The addition of APTES reduces the amount of water entering the pores and consequently the shift of L_α onset. As the capillary filling rate and condensation regime in the mesoporous films are not in direct correlation with the pore dimension and arrangement, as demonstrated by Ceratti et al. (2015), the effect of surfactant on the film preparation does not have big influence. Hydration can be partially tuned by playing with film treatment and surface functionalization.

The present results refer to POPC membranes deposited on the films by drop casting. Preliminary experiments on POPC deposited by dip coating showed the same behavior. However, further studies are required to investigate the effect of the POPC deposition method and of the resulting lipid membrane thickness on the hydration of supported lipid membranes on mesoporous silica substrates.

CONCLUSION

In the present work, we studied the hydration with RH increase of POPC lipid membranes supported on silicon and mesoporous silica films prepared with different surfactants, subject to diverse thermal treatment, and with and without surface functionalization with APTES. The contact angle was measured for every film prior to lipid membrane deposition. *In situ* GISAXS experiments were conducted in a humidity chamber on POPC deposited both on mesoporous materials and on bare silicon wafers with and without surface treatment with APTES. The hydration was examined by detecting the onset of the L_α phase of POPC (humid phase). It was found that the water uptake of the mesopores during RH increase leads to a hydration of the supported lipid membrane at a considerably lower RH with respect to the membrane deposited on bare silicon. The water uptake and the subsequent interaction with the lipid membrane can be partially tuned by using thermal treatment, to increase water adsorption and therefore hydration, and by functionalizing the surface with APTES for the opposite effect. The surfactant choice, leading to different dimensions and arrangement of the pores in the silica film, does not have a profound influence on POPC behavior.

The possibility of patterning the films, and a suitable surface functionalization of the mesopores with SAMs of different molecules with specific binding terminal groups could open the use of mesoporous films as "interactive" supports for biological studies of increasing complexity, such as protein/peptide incorporation for signaling. Thus, samples could be handled and modified from below and be investigated with different techniques from above.

The next step will be the investigation of the possibility of conveying liquids through the pores at constant RH by means of an appropriate reservoir. Studies of water delivery are already being conducted by our group using IR and GISAXS techniques.

DATA AVAILABILITY STATEMENT

The raw data supporting the conclusions of this article will be made available by the authors, without undue reservation.

AUTHOR CONTRIBUTIONS

BS participated in the synthesis and functionalization and in the GISAXS studies. IR and AK defined the surface functionalization protocol and performed CA measurements. HA and BM directed the project. HA participated in SAXS measurements. BM conducted the X-ray irradiation of the films and participated in GISAXS measurements. All authors contributed to the manuscript writing process.

ACKNOWLEDGMENTS

This research was partly supported by the European Commission under grant agreement 654360 NFFA-EUROPE. This work includes part of the scientific activities of the internal CERIC-ERIC project renewals. The authors are thankful to C. Morello and L. Sancin for their technical support. IR is grateful to the support of the Spanish Ministry of Economy and Competitiveness (MINECO) (PID2019-105622RBI00) through the Severo Ochoa Programme for Centres of Excellence in R&D (CEX 2019-000917-S), Instituto de Salud Carlos III through the Networking Research Center on Bioengineering, Biomaterials, and Nanomedicine (CIBER-BBN), Generalitat de Catalunya (SGR-918), and Fundacio Marato de TV3 (No. 201812).

SUPPLEMENTARY MATERIAL

The Supplementary Material for this article can be found online at: https://www.frontiersin.org/articles/10.3389/fmats.2021.686353/full#supplementary-material

REFERENCES

Amenitsch, H., Bernstorff, S., Kriechbaum, M., Lombardo, D., Mio, H., Rappolt, M., et al. (1997). Performance and First Results of the ELETTRA High-Flux Beamline for Small-Angle X-ray Scattering. *J. Appl. Cryst.* 30, 872–876. doi:10.1107/S0021889897001593

Amenitsch, H., Rappolt, M., Teixeira, C. V., Majerowicz, M., and Laggner, P. (2004). *In Situ* sensing of Salinity in Oriented Lipid Multilayers by Surface X-ray Scattering. *Langmuir* 20, 4621–4628. doi:10.1021/la036319p

Becker, E. W., Ehrfeld, W., Hagmann, P., Maner, A., and Münchmeyer, D. (1986). Fabrication of Microstructures with High Aspect Ratios and Great Structural Heights by Synchrotron Radiation Lithography, Galvanoforming, and Plastic Moulding (LIGA Process). *Microelectron. Eng.* 4, 35–56. doi:10.1016/0167-9317(86)90004-3

Bhattacharya, J., Kisner, A., Offenhäusser, A., and Wolfrum, B. (2011). Microfluidic Anodization of Aluminum Films for the Fabrication of Nanoporous Lipid Bilayer Support Structures. *Beilstein J. Nanotechnol.* 2, 104–109. doi:10.3762/bjnano.2.12

Bindini, E., Chehadi, Z., Faustini, M., Albouy, P.-A., Grosso, D., Cattoni, A., et al. (2020). Following *In Situ* the Degradation of Mesoporous Silica in Biorelevant Conditions: At Last, a Good Comprehension of the Structure Influence. *ACS Appl. Mater. Inter.* 12, 13598–13612. doi:10.1021/acsami.9b19956

Burian, M., Meisenbichler, C., Naumenko, D., and Amenitsch, H. (2020). *SAXSDOG: Open Software for Real-Time Azimuthal Integration of 2D Scattering Images*. 1–17. Available at: http://arxiv.org/abs/2007.02022 (Accessed July 4, 2020).

Calvo, A., Joselevich, M., Soler-Illia, G. J. A. A., and Williams, F. J. (2009). Chemical Reactivity of Amino-Functionalized Mesoporous Silica Thin Films Obtained by Co-condensation and post-grafting Routes. *Microporous Mesoporous Mater.* 121, 67–72. doi:10.1016/j.micromeso.2009.01.005

Ceratti, D. R., Faustini, M., Sinturel, C., Vayer, M., Dahirel, V., Jardat, M., et al. (2015). Critical Effect of Pore Characteristics on Capillary Infiltration in Mesoporous Films. *Nanoscale* 7, 5371–5382. doi:10.1039/C4NR03021D

Claesson, M., Cho, N.-J., Frank, C. W., and Andersson, M. (2010). Vesicle Adsorption on Mesoporous Silica and Titania. *Langmuir* 26, 16630–16633. doi:10.1021/la102719w

Claesson, M., Frost, R., Svedhem, S., and Andersson, M. (2011). Pore Spanning Lipid Bilayers on Mesoporous Silica Having Varying Pore Size. *Langmuir* 27, 8974–8982. doi:10.1021/la201411b

Craig, M., Jenner, A. L., Namgung, B., Lee, L. P., and Goldman, A. (2020). Engineering in Medicine to Address the Challenge of Cancer Drug Resistance: From Micro- and Nanotechnologies to Computational and Mathematical Modeling. *Chem. Rev.* 121, 3352–3389. doi:10.1021/acs.chemrev.0c00356

Crepaldi, E. L., Soler-Illia, G. J. d. A. A., Grosso, D., Cagnol, F., Ribot, F., and Sanchez, C. (2003). Controlled Formation of Highly Organized Mesoporous Titania Thin Films: From Mesostructured Hybrids to Mesoporous Nanoanatase TiO2. *J. Am. Chem. Soc.* 125, 9770–9786. doi:10.1021/ja030070g

Dourdain, S., and Gibaud, A. (2005). On the Capillary Condensation of Water in Mesoporous Silica Films Measured by X-ray Reflectivity. *Appl. Phys. Lett.* 87, 223105-3. doi:10.1063/1.2136412

Dourdain, S., Bardeau, J.-F., Colas, M., Smarsly, B., Mehdi, A., Ocko, B. M., et al. (2005). Determination by X-ray Reflectivity and Small Angle X-ray Scattering of the Porous Properties of Mesoporous Silica Thin Films. *Appl. Phys. Lett.* 86, 113108-3. doi:10.1063/1.1887821

Falcaro, P., Costacurta, S., Malfatti, L., Takahashi, M., Kidchob, T., Casula, M. F., et al. (2008). Fabrication of Mesoporous Functionalized Arrays by Integrating Deep X-ray Lithography with Dip-Pen Writing. *Adv. Mater.* 20, 1864–1869. doi:10.1002/adma.200702795

Falcaro, P., Malfatti, L., Vaccari, L., Amenitsch, H., Marmiroli, B., Grenci, G., et al. (2009). Fabrication of Advanced Functional Devices Combining Soft Chemistry with X-ray Lithography in One Step. *Adv. Mater.* 21, 4932–4936. doi:10.1002/adma.200901561

Fuertes, M. C., López-Alcaraz, F. J., Marchi, M. C., Troiani, H. E., Luca, V., Míguez, H., et al. (2007). Photonic Crystals from Ordered Mesoporous Thin-Film Functional Building Blocks. *Adv. Funct. Mater.* 17, 1247–1254. doi:10.1002/adfm.200601190

Ganser, C., Fritz-Popovski, G., Morak, R., Sharifi, P., Marmiroli, B., Sartori, B., et al. (2016). Cantilever Bending Based on Humidity-Actuated Mesoporous Silica/silicon Bilayers. *Beilstein J. Nanotechnol.* 7, 637–644. doi:10.3762/bjnano.7.56

Gibaud, A., Dourdain, S., Gang, O., and Ocko, B. M. (2004). In Situgrazing Incidence Small-Angle X-ray Scattering Real-Time Monitoring of the Role of Humidity during the Structural Formation of Templated Silica Thin Films. *Phys. Rev. B* 70, 1–4. doi:10.1103/PhysRevB.70.161403

Grosso, D., Cagnol, F., Soler-Illia, G. J. D. A. A., Crepaldi, E. L., Amenitsch, H., Brunet-Bruneau, A., et al. (2004). Fundamentals of Mesostructuring through Evaporation-Induced Self-Assembly. *Adv. Funct. Mater.* 14, 309–322. doi:10.1002/adfm.200305036

Huber, P. (2015). Soft Matter in Hard Confinement: Phase Transition Thermodynamics, Structure, Texture, Diffusion and Flow in Nanoporous media. *J. Phys. Condens. Matter* 27, 103102. doi:10.1088/0953-8984/27/10/103102

Innocenzi, P., and Malfatti, L. (2013). Mesoporous Thin Films: Properties and Applications. *Chem. Soc. Rev.* 42, 4198–4216. doi:10.1039/c3cs35377j

Innocenzi, P., Malfatti, L., Kidchob, T., Costacurta, S., Falcaro, P., Marmiroli, B., et al. (2011). Densification of Sol-Gel Silica Thin Films Induced by Hard X-Rays Generated by Synchrotron Radiation. *J. Synchrotron Radiat.* 18, 280–286. doi:10.1107/S0909049510051666

Innocenzi, P., Malfatti, L., Marmiroli, B., and Falcaro, P. (2014). Hard X-Rays and Soft-Matter: Processing of Sol-Gel Films from a Top Down Route. *J. Sol-gel Sci. Technol.* 70, 236–244. doi:10.1007/s10971-013-3227-y

Katsaras, J., Jeffrey, K. R., Yang, D. S. C., and Epand, R. M. (1993). Direct Evidence for the Partial Dehydration of Phosphatidylethanolamine Bilayers on Approaching the Hexagonal Phase. *Biochemistry* 32, 10700–10707. doi:10.1021/bi00091a021

Ketteler, G., Ashby, P., Mun, B. S., Ratera, I., Bluhm, H., Kasemo, B., et al. (2008). In Situphotoelectron Spectroscopy Study of Water Adsorption on Model Biomaterial Surfaces. *J. Phys. Condens. Matter* 20, 184024. doi:10.1088/0953-8984/20/18/184024

Khalil, A., Zimmermann, M., Bell, A. K., Kunz, U., Hardt, S., Kleebe, H.-J., et al. (2020). Insights into the Interplay of Wetting and Transport in Mesoporous Silica Films. *J. Colloid Interf. Sci.* 560, 369–378. doi:10.1016/j.jcis.2019.09.093

Kim, J., Kim, G., and Cremer, P. S. (2001). Investigations of Water Structure at the Solid/liquid Interface in the Presence of Supported Lipid Bilayers by Vibrational Sum Frequency Spectroscopy. *Langmuir* 17, 7255–7260. doi:10.1021/la0017274

Law, K.-Y. (2014). Definitions for Hydrophilicity, Hydrophobicity, and Superhydrophobicity: Getting the Basics Right. *J. Phys. Chem. Lett.* 5, 686–688. doi:10.1021/jz402762h

Lei, Q., Guo, J., Noureddine, A., Wang, A., Wuttke, S., Brinker, C. J., et al. (2020). Sol-Gel-Based Advanced Porous Silica Materials for Biomedical Applications. *Adv. Funct. Mater.* 30, 1–28. doi:10.1002/adfm.201909539

Leonenko, Z. V., Carnini, A., and Cramb, D. T. (2000). Supported Planar Bilayer Formation by Vesicle Fusion: The Interaction of Phospholipid Vesicles with Surfaces and the Effect of Gramicidin on Bilayer Properties Using Atomic Force Microscopy. *Biochim. Biophys. Acta (Bba) - Biomembr.* 1509, 131–147. doi:10.1016/S0005-2736(00)00288-1

Magner, E. (2013). Immobilisation of Enzymes on Mesoporous Silicate Materials. *Chem. Soc. Rev.* 42, 6213–6222. doi:10.1039/c2cs35450k

Mangold, H. K. (1995). *The Lipid Handbook*. Second Edition, F. D. Gunstone, J. L. Harwood, and F. B. Padley London: Chapman & HallLipid/Fett 97, 315–316. 1994Preis: £ 255. – (ISBN 0 412 43320 6). doi:10.1002/lipi.19950970720

Marmiroli, B., and Amenitsch, H. (2012). X-ray Lithography and Small-Angle X-ray Scattering: A Combination of Techniques Merging Biology and Materials Science. *Eur. Biophys. J.* 41, 851–861. doi:10.1007/s00249-012-0843-3

Milhaud, J. (2004). New Insights into Water-Phospholipid Model Membrane Interactions. *Biochim. Biophys. Acta (Bba) - Biomembr.* 1663, 19–51. doi:10.1016/j.bbamem.2004.02.003

Miyashita, W., Saeki, D., and Matsuyama, H. (2018). Formation of Supported Lipid Bilayers on Porous Polymeric Substrates Induced by Hydrophobic Interaction. *Colloids Surf. A: Physicochem. Eng. Aspects* 538, 297–303. doi:10.1016/j.colsurfa.2017.11.006

Pabst, G., Rappolt, M., Amenitsch, H., and Laggner, P. (2000). Structural Information from Multilamellar Liposomes at Full Hydration: Fullq-Range Fitting with High Quality X-ray Data. *Phys. Rev. E* 62, 4000–4009. doi:10.1103/PhysRevE.62.4000

Pérennès, F., De Bona, F., and Pantenburg, F. J. (2001). Deep X-Ray Lithography Beamline at ELETTRA. *Nucl. Instr. Methods Phys. Res.* 467–468, 1274–1278. doi:10.1016/S0168-9002(01)00632-5

Pérennès, F., and Pantenburg, F. J. (2001). Adhesion Improvement in the Deep X-ray Lithography Process Using a central Beam-Stop. *Nucl. Instr. Methods Phys. Res. Section B: Beam Interact.Mater. Atoms* 174, 317–323. doi:10.1016/S0168-583X(00)00588-7

Rappolt, M., Amenitsch, H., Strancar, J., Teixeira, C. V., Kriechbaum, M., Pabst, G., et al. (2004). Phospholipid Mesophases at Solid Interfaces: *In-Situ* X-ray Diffraction and Spin-Label Studies. *Adv. Colloid Interf. Sci.* 111, 63–77. doi:10.1016/j.cis.2004.07.004

Rappolt, M. (2010). Bilayer Thickness Estimations with "Poor" Diffraction Data. *J. Appl. Phys.* 107, 084701. doi:10.1063/1.3393600

Renaud, G., Lazzari, R., and Leroy, F. (2009). Probing Surface and Interface Morphology with Grazing Incidence Small Angle X-Ray Scattering. *Surf. Sci. Rep.* 64, 255–380. doi:10.1016/j.surfrep.2009.07.002

Romanato, F., Businaro, L., Tormen, M., Perennes, F., Matteucci, M., Marmiroli, B., et al. (2006). Fabrication of 3D Micro and Nanostructures for MEMS and MOEMS: An Approach Based on Combined Lithographies. *J. Phys. Conf. Ser.* 34, 904–911. doi:10.1088/1742-6596/34/1/150

Sánchez, G., Curiel, D., Ratera, I., Tárraga, A., Veciana, J., and Molina, P. (2013). Modified Mesoporous Silica Nanoparticles as a Reusable, Selective Chromogenic Sensor for Mercury(ii) Recognition. *Dalton Trans.* 42, 6318–6326. doi:10.1039/c2dt32243a

Scheler, O., Postek, W., and Garstecki, P. (2019). Recent Developments of Microfluidics as a Tool for Biotechnology and Microbiology. *Curr. Opin. Biotechnol.* 55, 60–67. doi:10.1016/j.copbio.2018.08.004

Seras-Franzoso, J., Díez-Gil, C., Vazquez, E., García-Fruitós, E., Cubarsi, R., Ratera, I., et al. (2012). Bioadhesiveness and Efficient Mechanotransduction Stimuli Synergistically provided by Bacterial Inclusion Bodies as Scaffolds for Tissue Engineering. *Nanomedicine* 7, 79–93. doi:10.2217/nnm.11.83

Sharifi, P., Marmiroli, B., Sartori, B., Cacho-Nerin, F., Keckes, J., Amenitsch, H., et al. (2014). Humidity-driven Deformation of Ordered Mesoporous Silica Films. *Bioinspired, Biomimetic Nanobiomater.* 3, 183–190. doi:10.1680/bbn.14.00017

Steinberg, P. Y., Lionello, D. F., Medone Acosta, D. E., Zalduendo, M. M., Amenitsch, H., Granja, L. P., et al. (2021). Structural and Mechanical Properties of Silica Mesoporous Films Synthesized Using Deep X-Rays: Implications in the Construction of Devices. *Front. Mater.* 8, 1–13. doi:10.3389/fmats.2021.628245

Sun, Y., Zang, X., Sun, Y., Wang, L., and Gao, Z. (2020). Lipid Membranes Supported by Planar Porous Substrates. *Chem. Phys. Lipids* 228, 104893. doi:10.1016/j.chemphyslip.2020.104893

Tatkiewicz, W. I., Seras-Franzoso, J., Garcia-Fruitos, E., Vazquez, E., Ventosa, N., Ratera, I., et al. (2013). 2D Engineering of Protein-Based Nanoparticles for Cell Guidance. *Tech. Proc. 2013 NSTI Nanotechnol. Conf. Expo. Nsti-nanotech 2013* 3, 229–231.

Tormen, M., Grenci, G., Marmiroli, B., and Romanato, F. (2013). *X-ray Lithography: Fundamentals and Applications*. Hoboken, NJ: John Wiley & Sons, Inc., 1–86. doi:10.1002/9781118622582.ch1

Tristram-Nagle, S., Zhang, R., Suter, R. M., Worthington, C. R., Sun, W. J., and Nagle, J. F. (1993). Measurement of Chain Tilt Angle in Fully Hydrated Bilayers of Gel Phase Lecithins. *Biophysical J.* 64, 1097–1109. doi:10.1016/S0006-3495(93)81475-9

Voss, G. J. B., Chavez Panduro, E. A., Midttveit, A., Fløystad, J. B., Høydalsvik, K., Gibaud, A., et al. (2014). Mesostructured Alumina as Powders and Thin Films. *J. Mater. Chem. A.* 2, 9727–9735. doi:10.1039/c4ta00604f

Xu, Y. (2018). Nanofluidics: A New Arena for Materials Science. *Adv. Mater.* 30, 1702419. doi:10.1002/adma.201702419

Yan, M., Henderson, M. J., and Gibaud, A. (2007). Grating Induced Micelle Alignment of Mesostructured Silica Films. *Appl. Phys. Lett.* 91, 023104–023105. doi:10.1063/1.2755722

Zhou, S., Guilfoil, E., He, Y., Nagpure, S., Islam, S. Z., Khan, M. A., et al. (2020). Nanoconfinement Effects on Redox Probe Transport in Lipid Assemblies on and in Mesoporous Silica Thin Films. *Adv. Mater. Inter.* 7, 1901787–1901789. doi:10.1002/admi.201901787

Conflict of Interest: The authors declare that the research was conducted in the absence of any commercial or financial relationships that could be construed as a potential conflict of interest.

Publisher's Note: All claims expressed in this article are solely those of the authors and do not necessarily represent those of their affiliated organizations, or those of the publisher, the editors and the reviewers. Any product that may be evaluated in this article, or claim that may be made by its manufacturer, is not guaranteed or endorsed by the publisher.